Electronic Supporting Information (ESI)

Supported Cu_3 Cluster on Graphitic Carbon Nitride as an Efficient Catalyst for CO Electroreduction to Propene

Yuting Sun,[a] Shuang Wang,[a] Jingjing Jia,[a] Yuejie Liu,[b,*] Qinghai Cai,[a,c] Jingxiang Zhao[a,*]

[a] *College of Chemistry and Chemical Engineering, Key Laboratory of Photonic and Electronic Bandgap Materials, Ministry of Education, Harbin Normal University, Harbin 150025, Heilongjiang, China*

[b] *Modern Experiment Center, Harbin Normal University, Harbin, 150025, China*

[c] *Heilongjiang Province Collaborative Innovation Center of Cold Region Ecological Safety, Harbin 150025, China*

[*] To whom correspondence should be addressed. Email: zjx1103@hotmail.com (YL) ; xjz_hmily@163.com or zhaojingxiang@hrbnu.edu.cn (JZ)

Computational Details of Dissolution Potential

To evaluate the stability of Cu_3@g-C_3N_4 monolayer in strong acidic media, we computed the dissolution potentials (U_{diss}, in V) of Cu in Cu_3@g-C_3N_4 at pH = 0, which was defined as: $U_{diss} = U_{Cu}^0 + \left[E_{Cu,bulk} - \left(E_{Cu_3@g-C_3N_4} - E_{d-Cu_3@g-C_3N_4}\right)\right]/ne$, where U_{Cu}^0 is the standard dissolution potential of Cu in the bulk form，d-Cu_3@g-C_3N_4 is the defective Cu_3@g-C_3N_4 monolayer by dissolving (removing) one Cu to solutions and *n* is the coefficient for the aqueous dissolution reaction: $Cu + 2H^+ \leftrightarrow Cu^{2+} + H_2$, namely, *n* equals to 2.

Table S1. The computed binding energies (E_{bind}), shortest distances between Cu clusters and g-C_3N_4, and the charges (Q) for various Cu_n (n=1-6) clusters anchored on g-C_3N_4.

	$Q(\|e\|)$							$d_{Cu\text{-}N}$	E_{bind}
	Cu_1	Cu_2	Cu_3	Cu_4	Cu_5	Cu_6	total	(Å)	(eV)
Cu_1@g-C_3N_4	0.74	—	—	—	—	—	0.74	2.18	-4.55
Cu_2@g-C_3N_4	0.41	0.44	—	—	—	—	0.85	1.95	-4.01
Cu_3@g-C_3N_4	0.31	0.31	0.31	—	—	—	0.94	2.03	-6.16
Cu_4@g-C_3N_4	0.40	0.42	0.41	-0.03	—	—	1.20	2.00	-7.86
Cu_5@g-C_3N_4	0.36	0.41	0.43	-0.10	0.02	—	1.12	2.00	-6.62
Cu_6@g-C_3N_4	0.41	0.41	0.42	-0.04	-0.03	-0.05	0.65	2.01	-6.28

Table S2. The computed free energy changes (Δ***G***, eV) of each possible elementary step for COER to generate CH_4 product on Cu_3@g-C_3N_4. The red represents higher selectivity.

Elementary step	Free energy change (ΔG)
$CO\ (g) + {}^{*} \rightarrow CO^{*}$	-0.98
$CO^{*} + H^{+} + e^{-} \rightarrow CHO^{*}$	0.45
$CO^{*} + H^{+} + e^{-} \rightarrow COH^{*}$	1.12
$CHO^{*} + H^{+} + e^{-} \rightarrow CH_2O^{*}$	0.03
$CHO^{*} + H^{+} + e^{-} \rightarrow CHOH^{*}$	0.45
$CH_2O^{*} + H^{+} + e^{-} \rightarrow CH_3O^{*}$	-0.63
$CH_2O^{*} + H^{+} + e^{-} \rightarrow CH_2OH^{*}$	-0.55
$CH_3O^{*} + H^{+} + e^{-} \rightarrow O^{*} + CH_4\ (g)$	-0.81
$CH_3O^{*} + H^{+} + e^{-} \rightarrow CH_3OH^{*}$	0.76
$O^{*} + H^{+} + e^{-} \rightarrow OH^{*}$	-0.33
$OH^{*} + H^{+} + e^{-} \rightarrow {}^{*} + H_2O$	0.37

Table S3. The computed free energy changes (Δ***G***, eV) of each possible elementary step for COER to generate C_3 product on Cu_3@g-C_3N_4. The red represents higher selectivity.

Elementary step	Free energy change (ΔG)
3CO (g) + * → CO-CO-CO*	-0.81
CO-CO-CO* + H^+ + e^- → CO-COH-CO*	-0.55
CO-CO-CO* + H^+ + e^- → CO-HCO-CO*	0.18
CO-COH-CO* + H^+ + e^- → CO-C-CO* + H_2O	-0.14
CO-COH-CO* + H^+ + e^- → COH-COH-CO*	0.03
CO-COH-CO* + H^+ + e^- → CHO-COH-CO*	0.31
CO-COH-CO* + H^+ + e^- → CO-HCOH-CO*	0.60
CO-COH-CO* + H^+ + e^- → CO-COH-COH*	0.05
CO-COH-CO* + H^+ + e^- → CO-COH-CHO*	0.33
CO-C-CO* + H^+ + e^- → CH-CO-CO*	-0.52
CO-C-CO* + H^+ + e^- → CHO-C-CO*	-0.44
CO-C-CO* + H^+ + e^- → COH-C-CO*	0.25
CO-C-CO* + H^+ + e^- → CO-C-COH*	0.12
CO-C-CO* + H^+ + e^- → CO-C-CHO*	-0.31
CH-CO-CO* + H^+ + e^- → CH-COH-CO*	-0.18
CH-CO-CO* + H^+ + e^- → CH_2-CO-CO*	0.02
CH-CO-CO* + H^+ + e^- → CH-CHO-CO*	0.07
CH-CO-CO* + H^+ + e^- → CH-CO-CHO*	0.27
CH-CO-CO* + H^+ + e^- → CH-CO-COH*	0.18
CH-COH-CO* + H^+ + e^- → CH-COH-CHO*	-0.20
CH-COH-CO* + H^+ + e^- → CH_2-COH-CO*	-0.06
CH-COH-CO* + H^+ + e^- → CH-C-CO* + H_2O	0.25
CH-COH-CO* + H^+ + e^- → CH-HCOH-CO*	0.77
CH-COH-CO* + H^+ + e^- → CH-COH-COH*	-0.02
CH-COH-CHO* + H^+ + e^- → CH-C-CHO*+ H_2O	-0.10
CH-COH-CHO* + H^+ + e^- → CH_2-COH-CHO*	0.50
CH-COH-CHO* + H^+ + e^- → CH-HCOH-CHO*	1.11
CH-COH-CHO* + H^+ + e^- → CH-COH-CHOH*	0.44
CH-COH-CHO* + H^+ + e^- → CH-COH-CH_2O^*	1.15
CH-C-CHO* + H^+ + e^- → CH_2-C-CHO*	-0.12

$CH\text{-}C\text{-}CHO^{*} + H^{+} + e^{-} \rightarrow CH\text{-}CH\text{-}CHO^{*}$	0.09
$CH\text{-}C\text{-}CHO^{*} + H^{+} + e^{-} \rightarrow CH\text{-}C\text{-}CHOH^{*}$	0.11
$CH\text{-}C\text{-}CHO^{*} + H^{+} + e^{-} \rightarrow CH\text{-}C\text{-}CH_2O^{*}$	1.12
$CH_2\text{-}C\text{-}CHO^{*} + H^{+} + e^{-} \rightarrow CH_3\text{-}C\text{-}CHO^{*}$	-0.34
$CH_2\text{-}C\text{-}CHO^{*} + H^{+} + e^{-} \rightarrow CH_2\text{-}CH\text{-}CHO^{*}$	-0.15
$CH_2\text{-}C\text{-}CHO^{*} + H^{+} + e^{-} \rightarrow CH_2\text{-}C\text{-}CHOH^{*}$	0.06
$CH_2\text{-}C\text{-}CHO^{*} + H^{+} + e^{-} \rightarrow CH_2\text{-}C\text{-}CH_2O^{*}$	-0.09
$CH_3\text{-}C\text{-}CHO^{*} + H^{+} + e^{-} \rightarrow CH_3\text{-}C\text{-}CHOH^{*}$	-0.09
$CH_3\text{-}C\text{-}CHO^{*} + H^{+} + e^{-} \rightarrow CH_3\text{-}CH\text{-}CHO^{*}$	0.17
$CH_3\text{-}C\text{-}CHO^{*} + H^{+} + e^{-} \rightarrow CH_3\text{-}C\text{-}CH_2O^{*}$	0.61
$CH_3\text{-}C\text{-}CHOH^{*} + H^{+} + e^{-} \rightarrow CH_3\text{-}C\text{-}CH^{*} + H_2O$	-0.66
$CH_3\text{-}C\text{-}CHOH^{*} + H^{+} + e^{-} \rightarrow CH_3\text{-}CH\text{-}CHOH^{*}$	0.25
$CH_3\text{-}C\text{-}CHOH^{*} + H^{+} + e^{-} \rightarrow CH_3\text{-}C\text{-}CH_2OH^{*}$	0.42
$CH_3\text{-}C\text{-}CH^{*} + H^{+} + e^{-} \rightarrow CH_3\text{-}CH\text{-}CH^{*}$	-0.51
$CH_3\text{-}C\text{-}CH^{*} + H^{+} + e^{-} \rightarrow CH_3\text{-}C\text{-}CH_2{}^{*}$	-0.36
$CH_3\text{-}CH\text{-}CH^{*} + H^{+} + e^{-} \rightarrow CH_3\text{-}CH\text{-}CH_2{}^{*}$	0.40
$CH_3\text{-}CH\text{-}CH^{*} + H^{+} + e^{-} \rightarrow CH_3\text{-}CH_2\text{-}CH^{*}$	0.51
$CH_3\text{-}CH\text{-}CH_2{}^{*} \rightarrow CH_3\text{-}CH\text{-}CH_2 + {}^{*}$	0.48

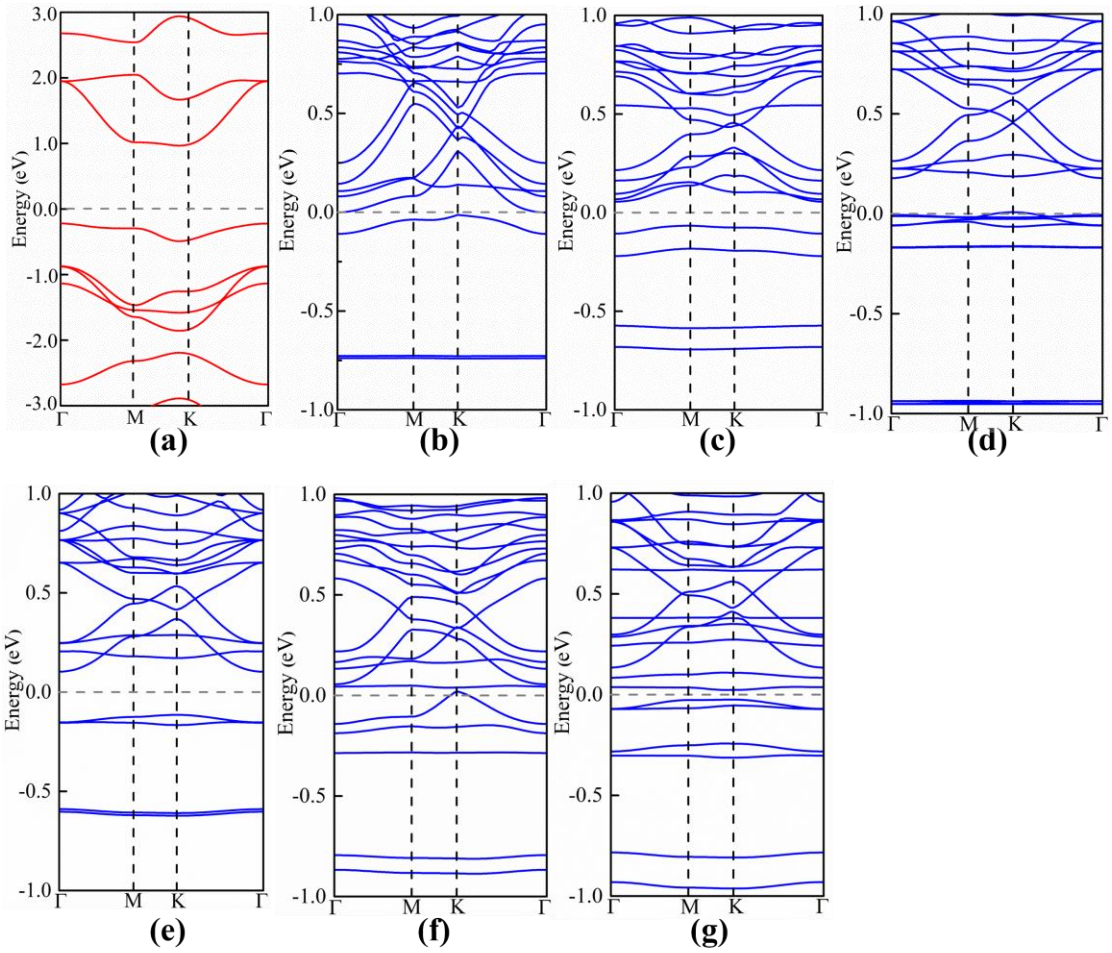

Fig. S1. The computed band structure for (a) the pristine g-C_3N_4, (b) Cu_1@g-C_3N_4, (c) Cu_2@g-C_3N_4, (d) Cu_3@g-C_3N_4, (e) Cu_4@g-C_3N_4, (f) Cu_5@g-C_3N_4 and (g) Cu_6@g-C_3N_4. The Fermi level was set to zero in dottedl line.

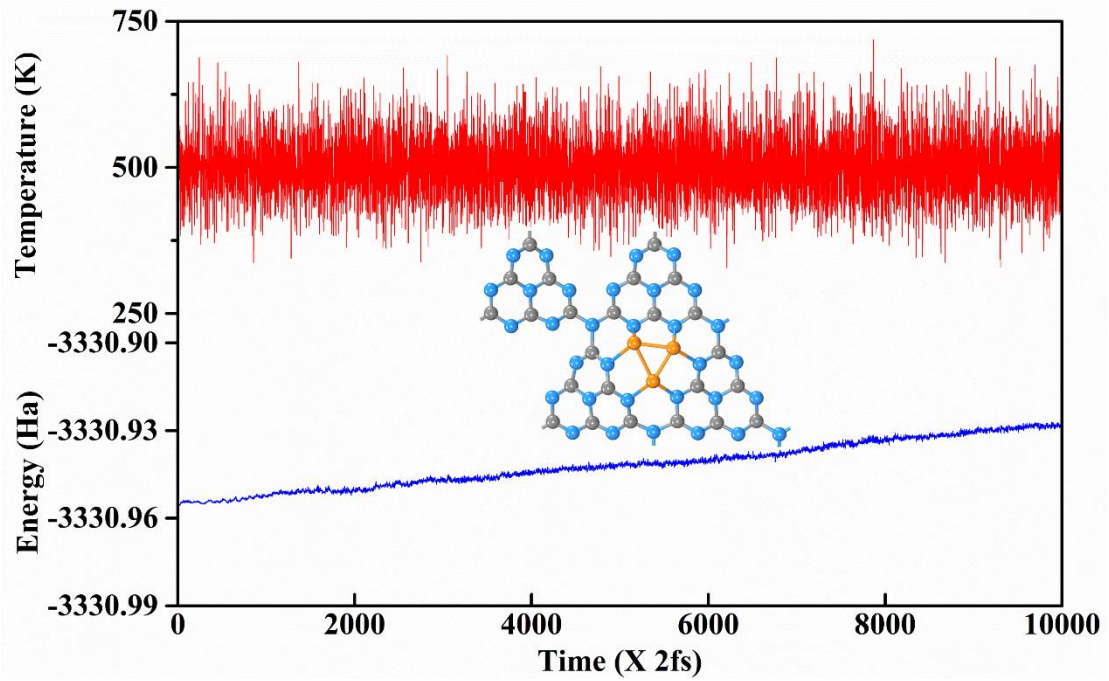

Fig. S2. Variations of temperature and energy as a function of the time for AIMD simulations of Cu_3@g-C_3N_4; insert is top view of the snapshot of atomic configuration. The simulation is run under 500 K for 20 ps with a time step of 2 fs. Gray, blue and orange spheres represent the C, N and Cu atoms, respectively.

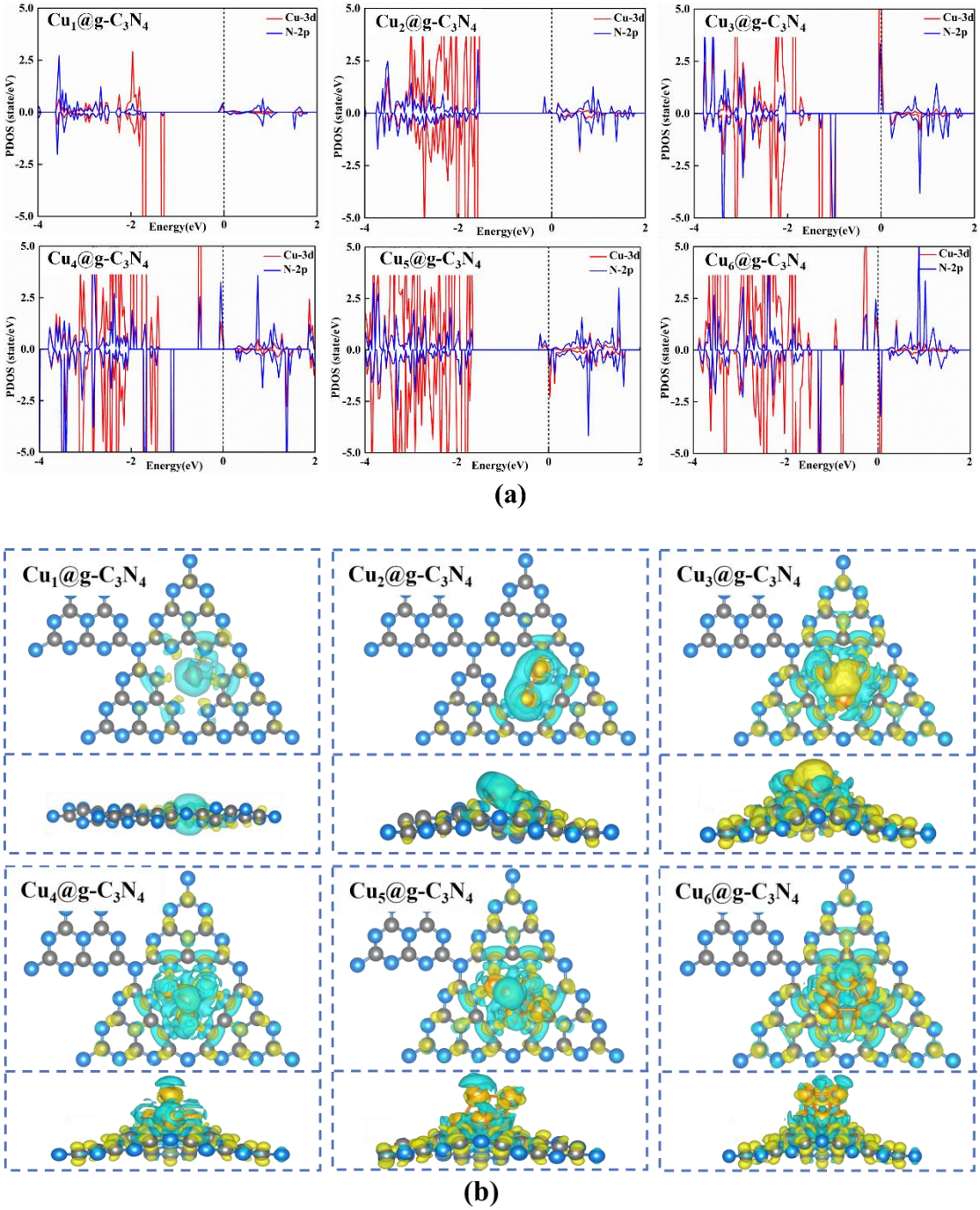

Fig. S3. (a) The projected density of states (PDOSs) between Cu-3d and N-2p orbitals for Cu_n@g-C_3N_4 (n = 1~6) monolayer, and the Fermi level was set to zero in dotted line. (b) Charge density differences of Cu_n@g-C_3N_4 (n = 1~6). The cyan and yellow regions refer to electron depletion regions and accumulation. The isosurface values were set as 0.003 eV $Å^{-3}$.

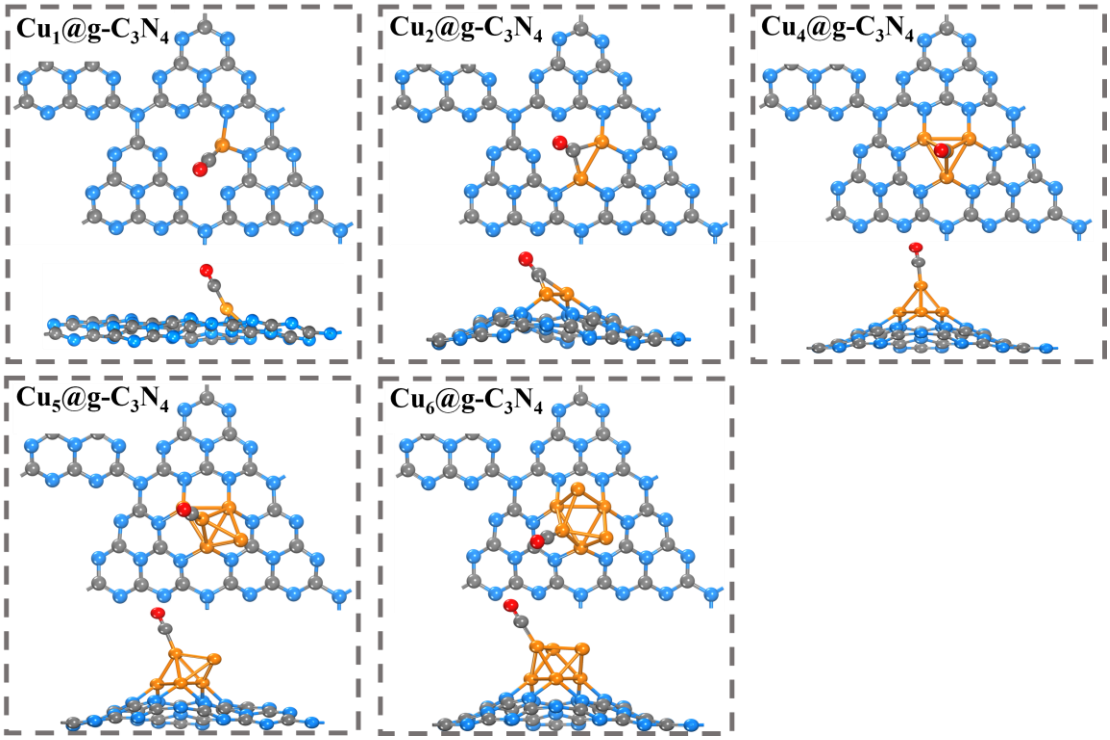

Fig. S4. The optimized most stable configurations for the adsorption of CO molecule on Cu_n@g-C_3N_4 (n = 1-2 and 4-6). The gray, blue, orange and red balls represent C, N, Cu and O atoms, respectively.

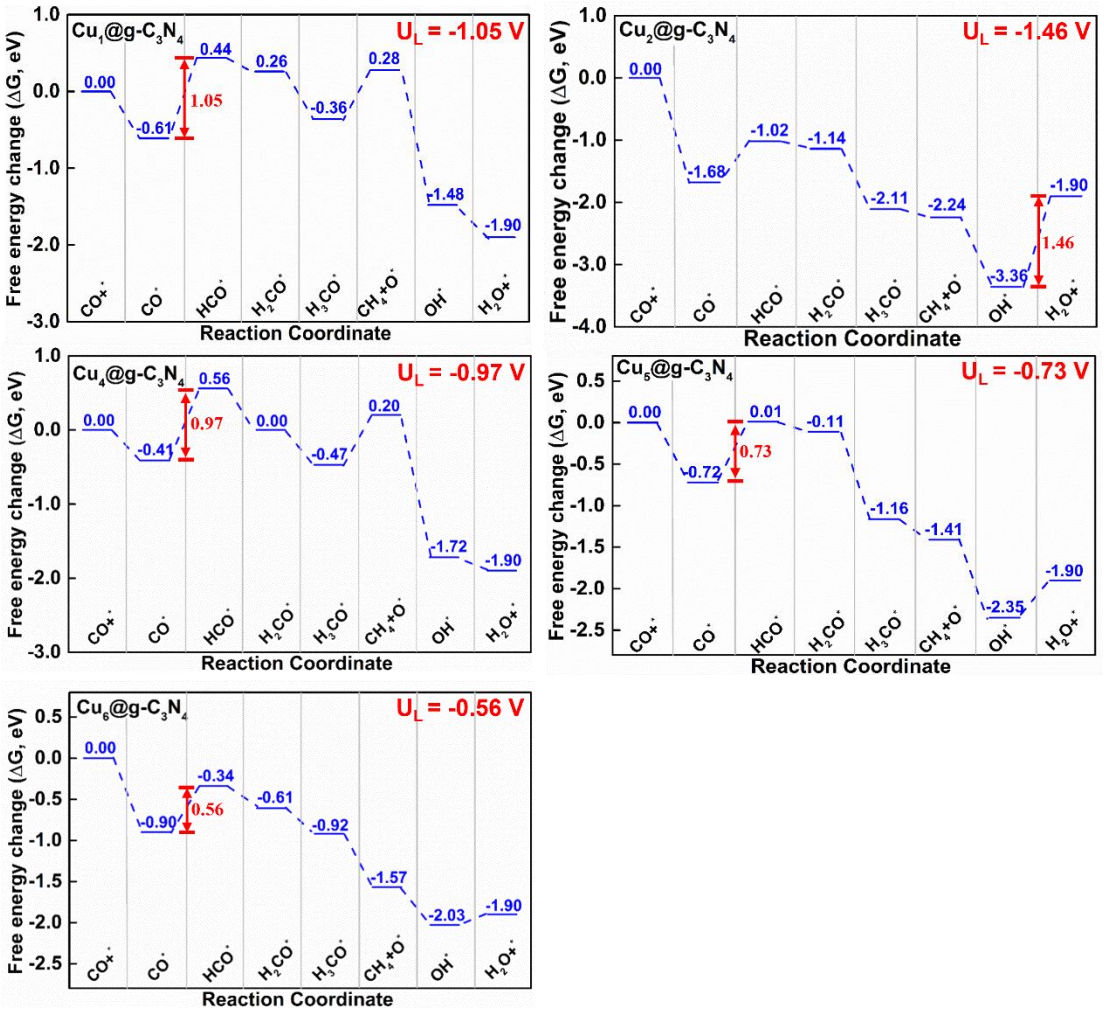

Fig. S5. Free energy diagrams for COER on Cu_n@g-C_3N_4 (n = 1-2 and 4-6).

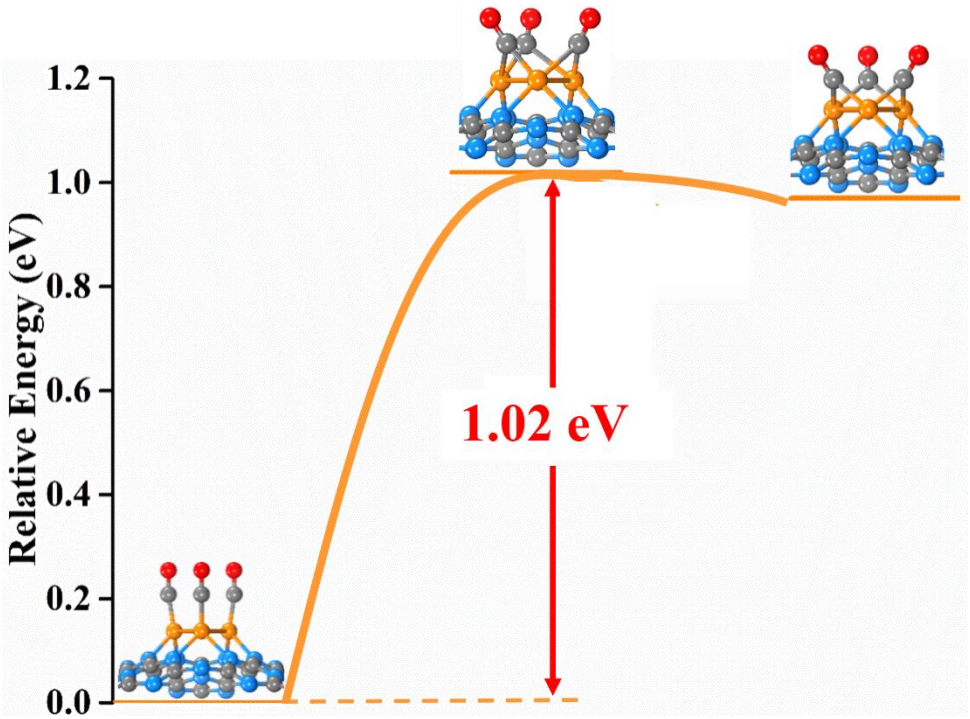

Fig. S6. The minimum pathway and the corresponding atomic configurations for the transformation from α-3CO* to β-3CO*.

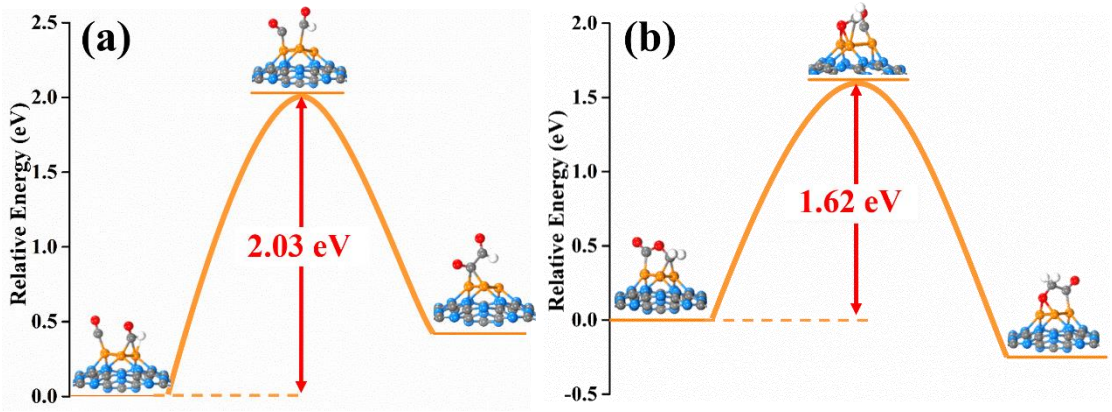

Fig. S7. The computed minimum pathways and the involved atomic configurations for (a) the coupling between CO^* and CHO^* and (b) the coupling between CO^* and CH_2O^*. The gray, blue, orange, red, and white balls represent C, N, Cu, O and H atoms, respectively.

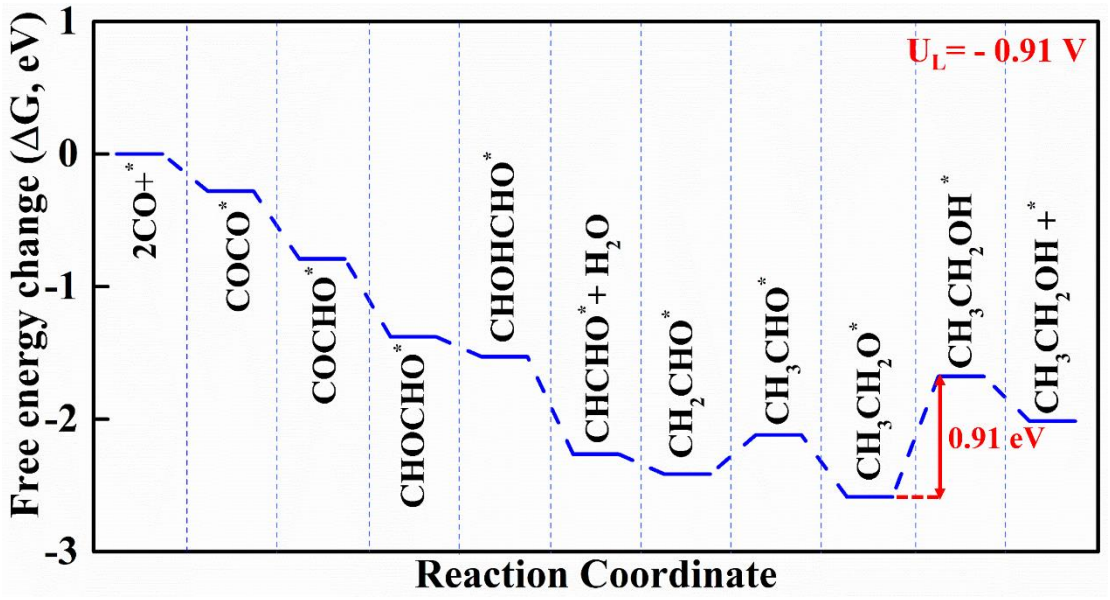

Fig. S8. The most energetically favorable reaction pathway for COER to generate C_2 products (ethanol) on Cu_3@g-C_3N_4.